Supplement.

S1. Allan variance plots

S2. Water correction plots

S3. Calibration factors

S4. Flight survey details

S5. Controlled release details and corresponding UAV aerial flight tracks

S6. Wind profiles and uncertainties

S7. Testing flux results

S1 Allan variance plots

An Allan variance precision test was performed on both the MGGA and the pMGGA using dry air from a gas cylinder. The MGGA sampled the cylinder for 17 hours and 23 minutes of continuous uninterrupted sampling, while the pMGGA sampled the cylinder for 38 hours and 30 minutes of continuous uninterrupted sampling. Mole fraction measurements from both instruments were corrected by applying their respective gain factors, given in Table 2. The Allan variance was calculated for each data set, as a function of integration time. The Allan variance plot for the MGGA is given in Figure S1 and Allan variance plot for the pMGGA is given in Figure S2.

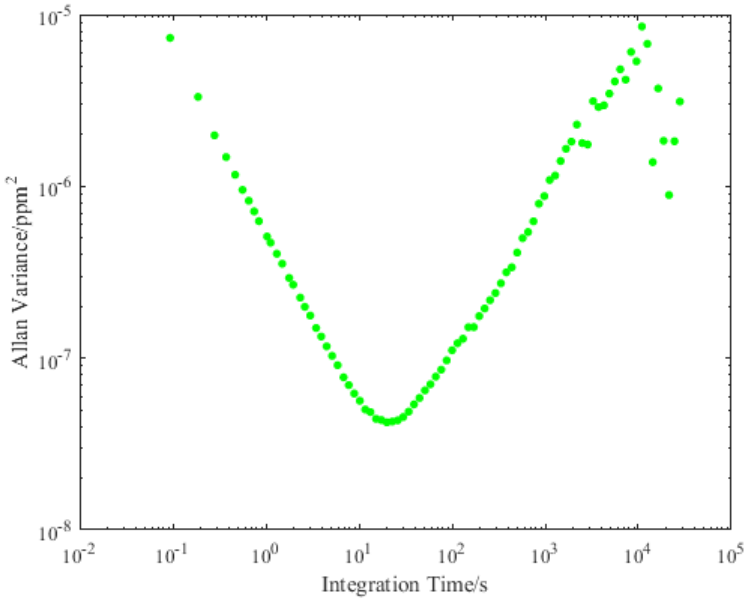

Figure S1. Allan variance plot for the MGGA plotted against integration time on logarithmic axes.

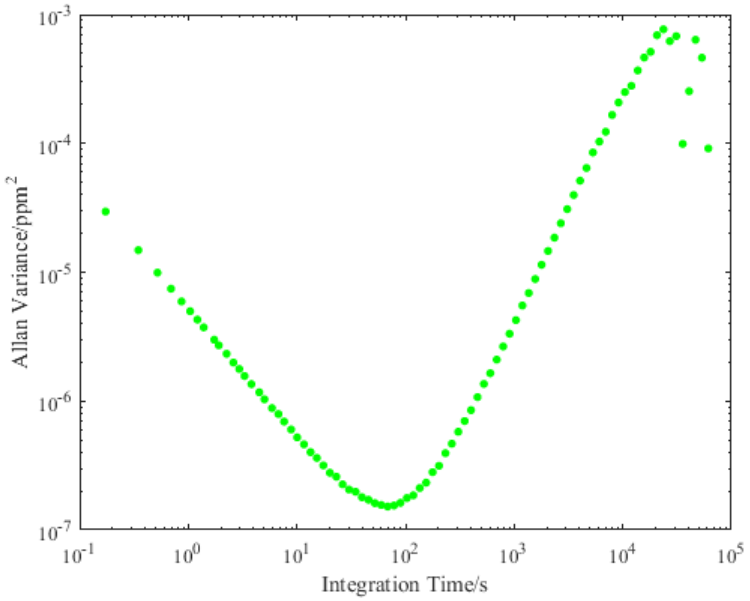

Figure S2. Allan variance plot for the pMGGA plotted against integration time on logarithmic axes.

S2 Water correction plots

$[H_2O]_0$ was required for both instruments, in order to derive *v*. $[H_2O]_0$ could be modelled using Eq. (1), by fitting $[X]_0^{dry}$ to $[H_2O]_0$. The measured and fitted $[H_2O]_0$ values as a function of $[X]_0^{dry}$ for the MGGA are given in Figure S3 and for the pMGGA are given in Figure S4.

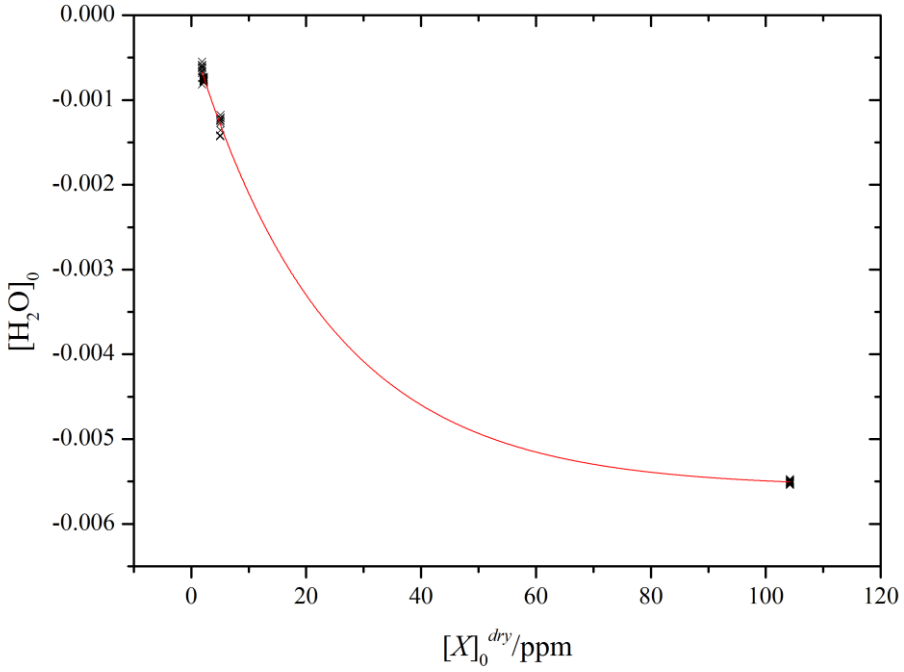

Figure S3. Measured water mole fraction offset as a function of $[X]_0^{dry}$ (black crosses) with a corresponding exponential decay function fit (red line) for the MGGA.

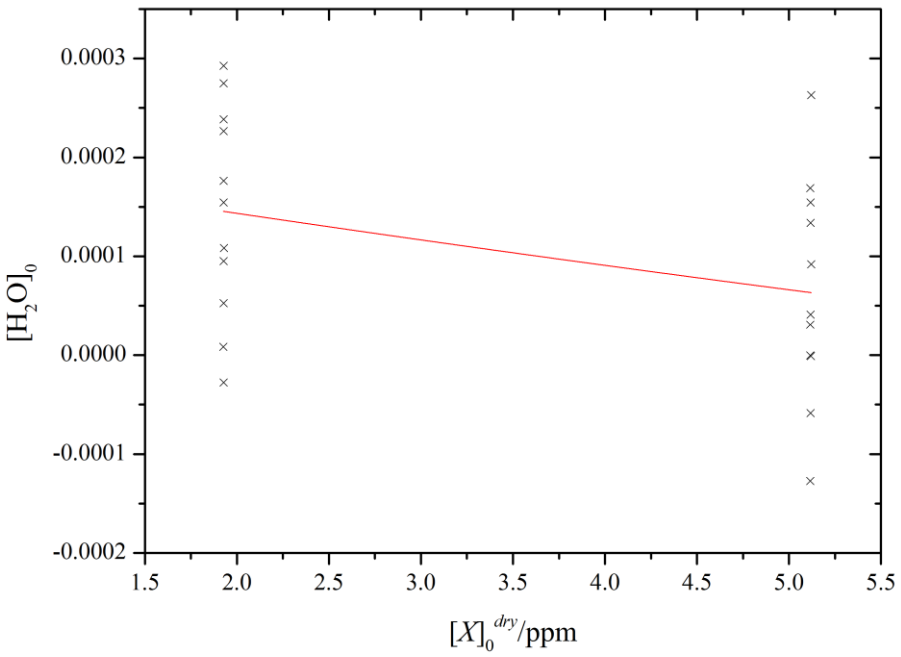

Figure S4. Measured water mole fraction offset as a function of $[X]_0^{dry}$ (black crosses) with a corresponding exponential decay function fit (red line) for the pMGGA.

Each water correction factor, as a function of [H_2O], was calculated by sampling a humidified gas which was either dried or fed directly into the MGGA or pMGGA without drying it. An example of $[X]_0$ during the transition between dry to wet sample gas, used to derive a *v* point, in shown in Figure S6. After the humidity of the air was adjusted, the gas was sampled dry for 5 minutes, from which measurements from the final 4 minutes were taken. The gas was then sampled wet for 8 minutes, from which measurements from the final 2 minutes were taken. The gas was then sampled dry for five minutes to ensure that $[X]_0$ returned to its original dry value.

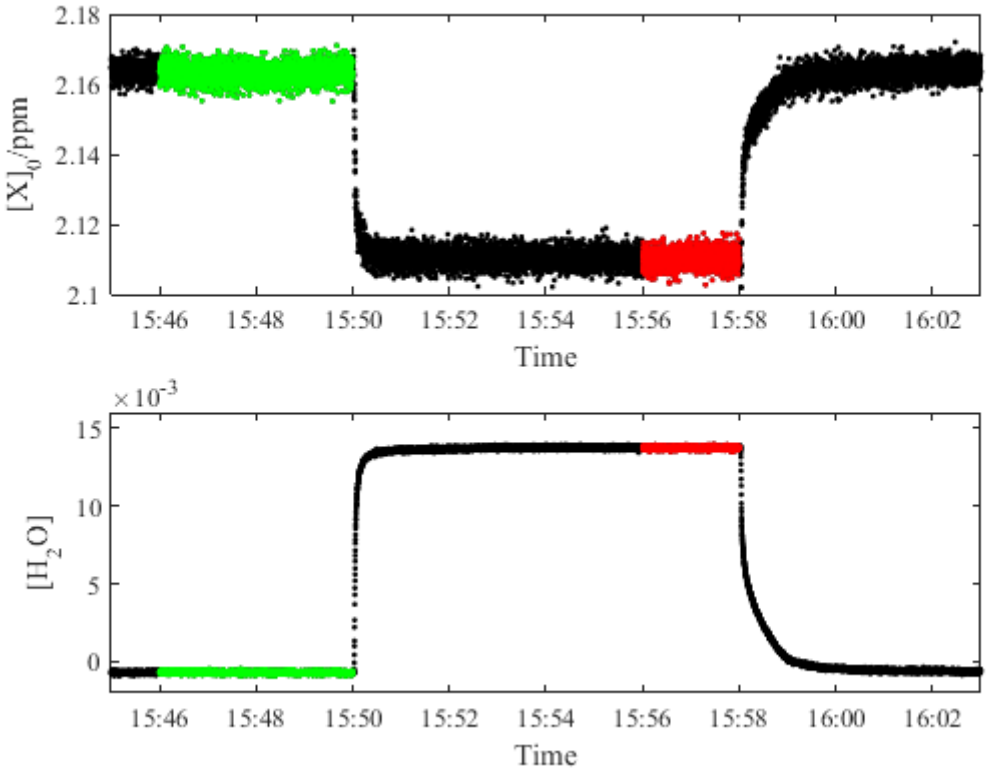

Figure S5. Uncalibrated methane mole fraction measurements (upper panel) and corresponding water mole fraction measurements (lower panel) made by the MGGA when transitioning between dry and wet gas at a dew point of 16° C. Red dots indicate measurements used to calculate $[X]_0$ and green dots indicate measurements used to calculate $[X]_0^{dry}$.

The water correction factor was plotted as a function of $[H_2O]$, corrected by the water offset, for the MGGA in Figure S6 and for the pMGGA in Figure S7. The data was fitted to Eq. (2) to derive the water correction parameters in Table 2. The residuals from the fit were used to derive σ_v, for each instrument.

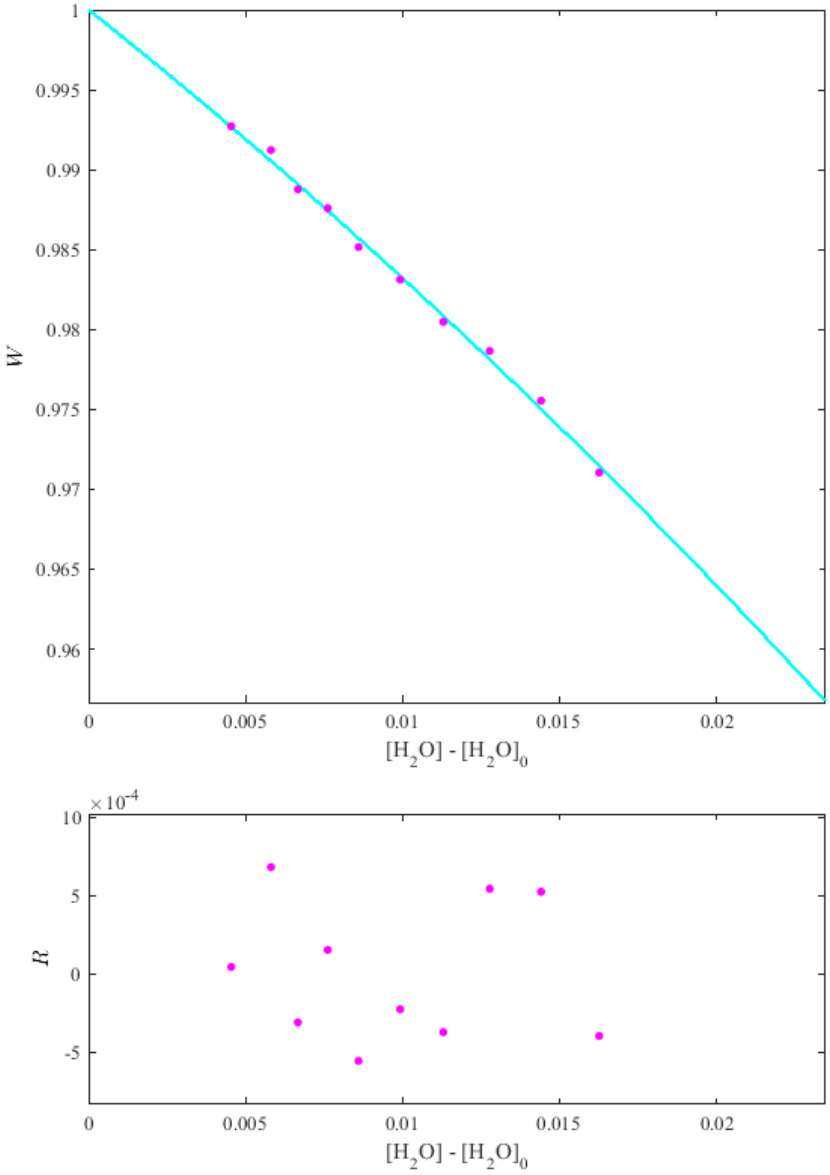

Figure S6. The water correction factor (upper panel) plotted as a function of baseline corrected water mole fraction (magenta dots) for the MGGA. The cyan line is a polynomial fit to the data, given by Eq. (2). v **is** $[X]_0$ **divided by** $[X]_0^{dry}$**, measured by the instrument. Corresponding residuals are given (lower panel) as magenta dots.**

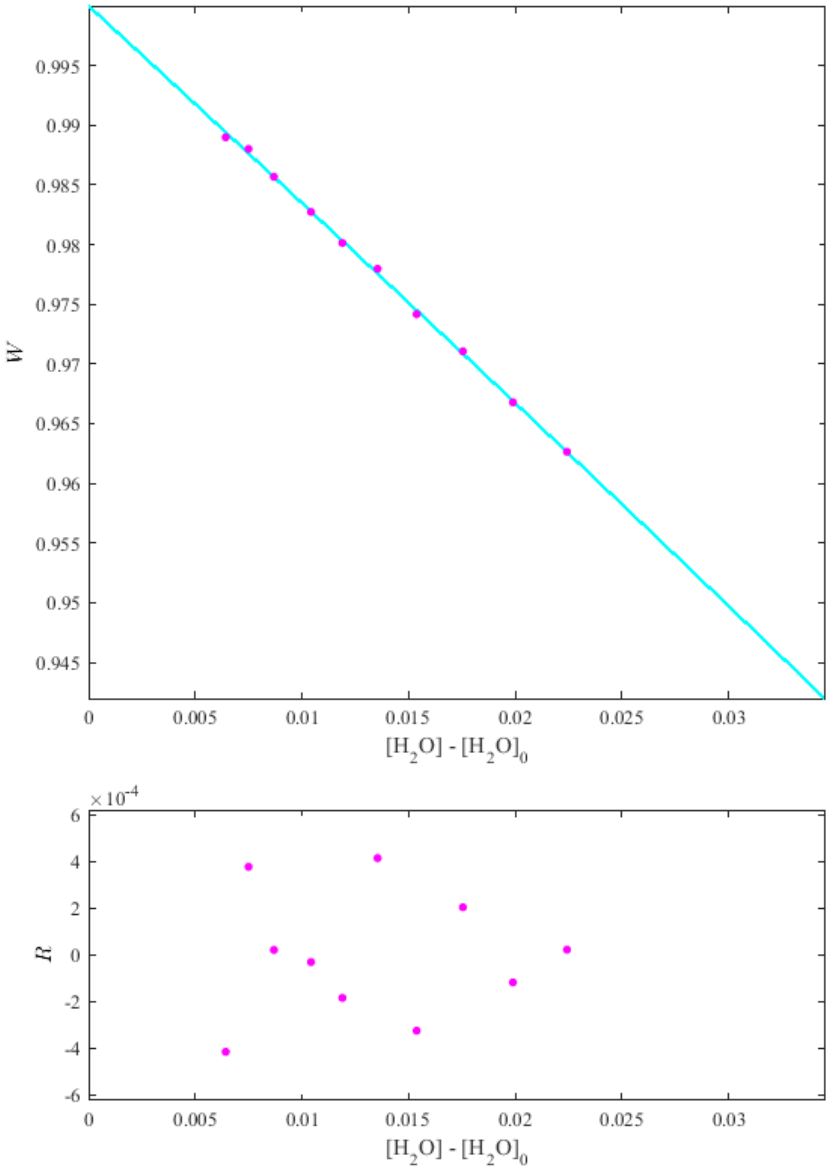

Figure S7. The water correction factor (upper panel) plotted as a function of baseline corrected water mole fraction (magenta dots) for the pMGGA. The cyan line is a polynomial fit to the data, given by Eq. (2). v **is** $[X]_0$ **divided by** $[X]_0^{dry}$**, measured by the instrument. Corresponding residuals are given (lower panel) as magenta dots.**

S3 Calibration factors

In order to calculate G for each instrument, interpolated values of $[X]_0^{dry}{}_{low}$ and $[X]_0^{dry}{}_{high}$ were generated to match measured values of $[X]_0^{dry}{}_{low}$ and $[X]_0^{dry}{}_{high}$, using a piecewise cubic hermite interpolating polynomial on MATLAB R2016a. Each interpolated value of $[X]_0^{dry}{}_{low}$ and $[X]_0^{dry}{}_{high}$ was generated using measured values 4 minutes before and after the point of interpolation. These interpolated and measured $[X]_0^{dry}{}_{low}$ and $[X]_0^{dry}{}_{high}$ values are given in Figure S8 and Figure S9 for the MGGA and pMGGA, respectively. The difference between $[X]_0^{dry}{}_{low}$ and $[X]_0^{dry}{}_{high}$ at each measurement point was used to calculate individual gain factors using Eq. (6). The gain factors can then be used to calculate individual offsets using Eq. (7) and Eq. (8). All individual gain factors and offsets are plotted in are given in Figure S8 and Figure S9.

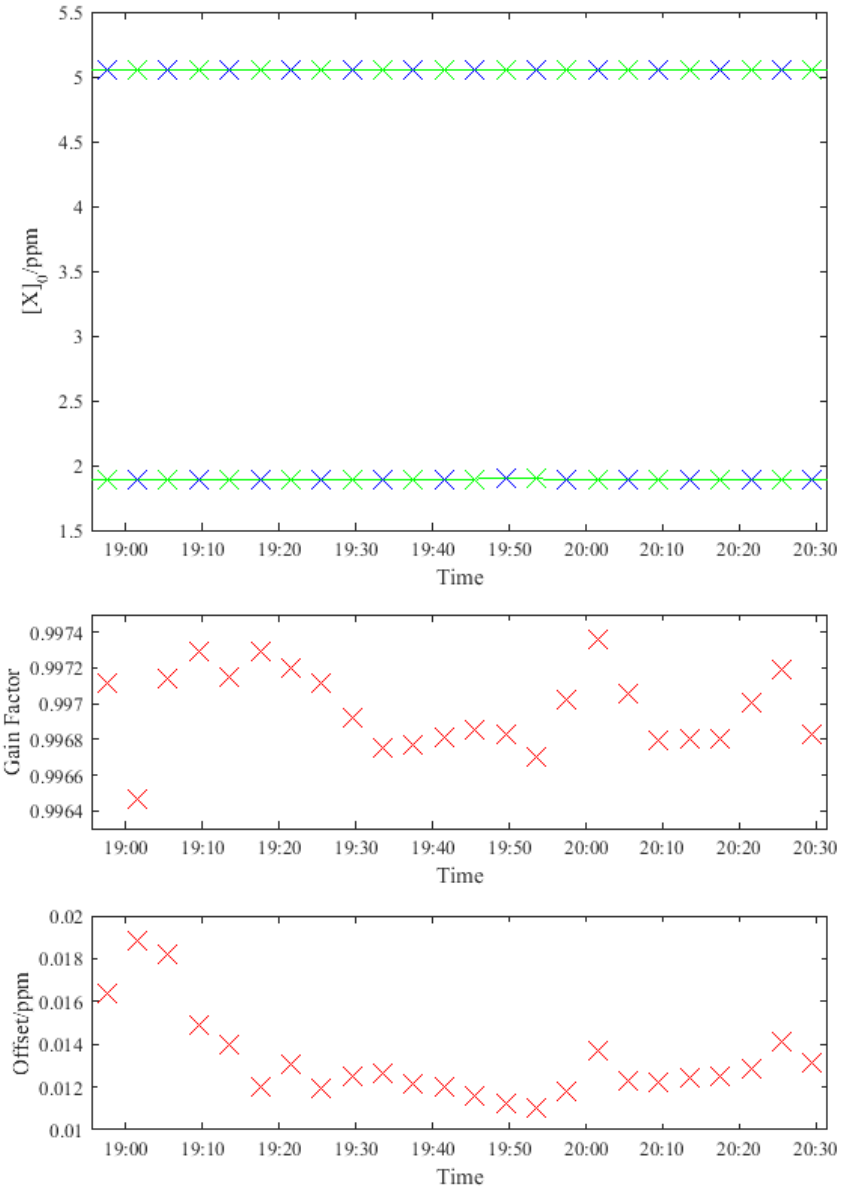

Figure S8. Measured $[X]_0^{dry}{}_{low}$ and $[X]_0^{dry}{}_{high}$ values (upper panel) as blue crosses and interpolated $[X]_0^{dry}{}_{low}$ and $[X]_0^{dry}{}_{high}$ values as green crosses for the MGGA. The interpolation curves (green line) are also given. The middle panel shows corresponding individual gain factors and the lower panel shows corresponding offsets.

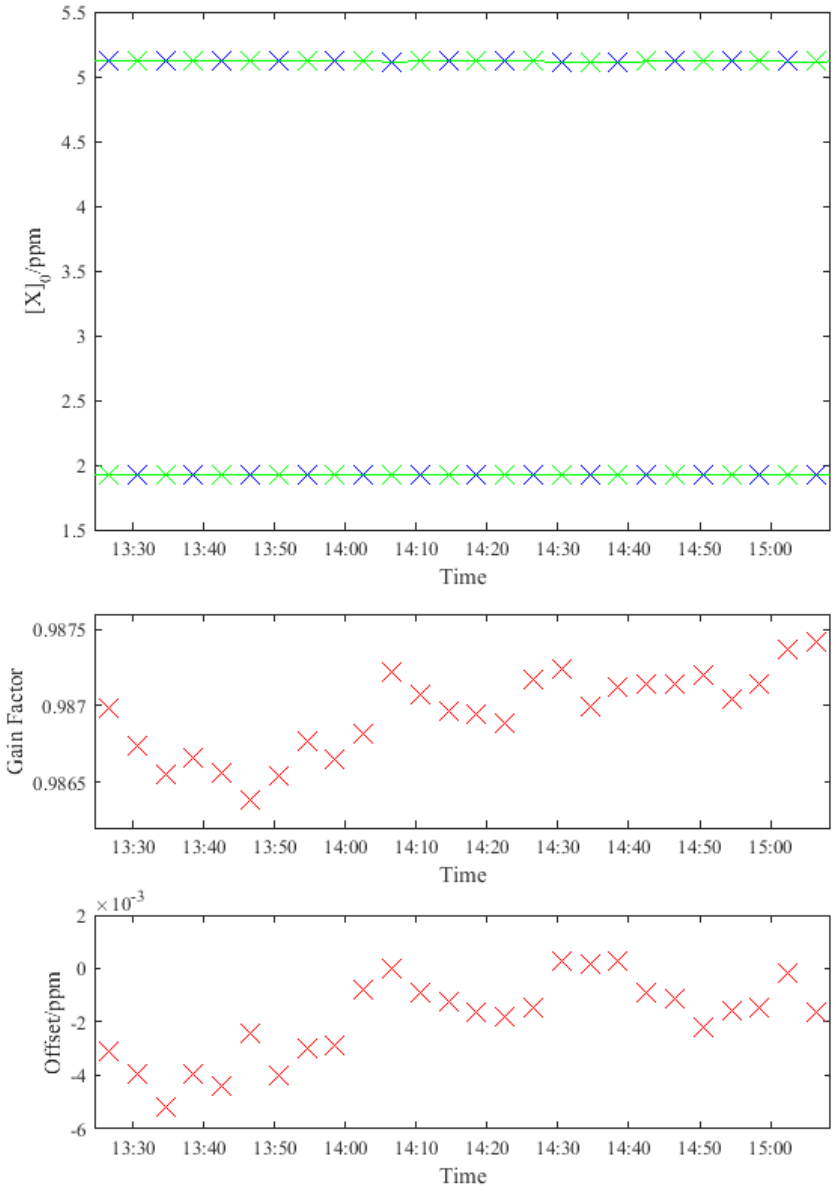

Figure S9. Measured $[X]_0^{dry}{}_{low}$ and $[X]_0^{dry}{}_{high}$ values (upper panel) as blue crosses and interpolated $[X]_0^{dry}{}_{low}$ and $[X]_0^{dry}{}_{high}$ values as green crosses for the pMGGA. The interpolation curves (green line) are also given. The middle panel shows corresponding individual gain factors and the lower panel shows corresponding offsets.

S4 Flight survey details

The duration of each flight survey, during which $[X]_0$ measurements were used, are given in Table S1 and Table S2, for UAV1 and UAV2, respectively, during method testing. Sampling periods in which there were kinks have been omitted from Table S1 for UAV1. The weighted average parallel distance (x_0) is also given. This represents the parallel distance of the sampling plane from the source, weighted to the position of enhancements in E across the sampling plane (see Shah et al. (2019)). The average spatial velocity of each UAV is also given in Table S1 and Table S2 which represents the velocity of the UAV as it travels across the sampling plane for the duration of $[X]_0$ measurement acquisition.

Flight survey (colour in Figure S10)	**Date**	**Controlled release number (position on Figure 1)**	**Start time**	**End time**	**Duration/s**	**Full duration/s**	**Spatial velocity/ m s^{-1}**	**x_0/m**	**$\overline{u(3.3)}$/m s^{-1}**	**$\overline{v(3.3)}$/m s^{-1}**
T1.1 (red)	21.8. 2018	C.3 (A)	15:31:45	15:34:15	150	456	1.47	50.8	+3.6 ±0.6	+0.5 ±0.7
			15:35:35	15:35:43	9					
			15:36:35	15:37:53	78					
			15:42:48	15:45:02	134					
			15:46:35	15:48:00	85					
T1.2 (red)	23.8. 2018	C.8 (C)	11:21:02	11:26:26	324	619	1.41	48.0	+4.8 ±0.6	+1.8 ±0.9
			11:31:39	11:36:34	295					
T1.3 (green)	23.8. 2018	C.9 (C)	13:08:17	13:11:11	174	480	1.47	48.6	+5.9 ±0.8	+3.9 ±1.1
			13:12:05	13:13:04	59					
			13:18:21	13:22:29	248					
T1.4 (red)	3.9. 2018	C.10 (D)	14:05:05	14:09:58	293	435	1.46	49.9	+5.1 ±0.1	-2.9 ±1.0
			14:15:27	14:17:18	111					
			14:18:50	14:19:06	17					
			14:20:14	14:20:28	14					
T1.5 (green)	3.9. 2018	C.11 (D)	15:05:17	15:06:40	83	577	1.57	50.4	+3.7 ±0.6	-3.5 ±0.7
			15:07:47	15:11:11	204					
			15:19:22	15:24:12	290					
T1.6 (blue)	3.9. 2018	C.12 (D)	16:10:31	16:15:31	300	541	1.50	49.2	+3.7 ±0.7	-1.9 ±0.6
			16:25:42	16:27:25	103					
			16:29:48	16:32:06	138					
T1.7 (red)	4.9. 2018	C.13 (E)	11:52:16	11:57:10	294	522	1.64	49.3	-0.3 ±0.7	-2.6 ±0.5
			12:05:43	12:09:31	228					

Table S1: UAV1 flight survey details during method testing. Periods of kinking of the tubing have been isolated. The position of the controlled release corresponding to each flight survey is given in brackets after the controlled release number.

Flight survey (colour in Figure S11)	Date	Controlled release number (position on Figure 1)	Start time	End time	Full duration/s	UAV1 *P* value used from Table S4	Spatial velocity/ m s^{-1}	x_0/m	$\overline{u(3.3)}$/m s^{-1}	$\overline{v(3.3)}$/m s^{-1}
T2.1 (red)	21.8. 2018	C.1 (A)	13:22:35	13:30:00	445	T1.3	3.32	104.0	+3.1 ±1.1	+0.5 ±1.0
T2.2 (green)	21.8. 2018	C.2 (A)	14:01:17	14:09:06	469	T1.3	2.76	101.6	+3.2 ±0.7	+1.0 ±0.6
T2.3 (blue)	21.8. 2018	C.2 (A)	14:17:15	14:24:52	457	T1.3	3.77	109.6	+3.2 ±0.9	-0.2 ±0.8
T2.4 (cyan)	21.8. 2018	C.3 (A)	15:29:54	15:38:24	510	T1.3	3.56	96.9	+3.6 ±0.6	-0.6 ±0.8
T2.5 (magenta)	21.8. 2018	C.3 (A)	15:43:57	15:52:59	542	T1.3	2.98	99.3	+3.4 ±0.3	+0.7 ±0.4
T2.6 (red)	22.8. 2018	C.4 (B)	10:01:24	10:09:22	478	T1.5	2.27	57.9	+2.4 ±1.0	+3.9 ±0.7
T2.7 (green)	22.8. 2018	C.5 (B)	10:31:18	10:38:25	427	T1.5	2.53	63.7	+3.7 ±0.9	+3.7 ±1.3
T2.8 (blue)	22.8. 2018	C.6 (B)	11:28:09	11:35:44	456	T1.5	1.28	113.7	+4.3 ±0.6	+4.3 ±1.6
T2.9 (cyan)	22.8. 2018	C.7 (B)	12:30:33	12:41:04	631	T1.5	1.75	86.7	+5.2 ±1.2	+4.5 ±1.1
T2.10 (red)	23.8. 2018	C.8 (C)	10:40:15	10:47:15	420	T1.4	2.57	97.4	+5.2 ±1.3	+1.9 ±0.8
T2.11 (green)	23.8. 2018	C.8 (C)	10:55:04	11:01:38	394	T1.4	2.70	95.0	+4.4 ±1.2	+1.5 ±0.6
T2.12 (blue)	23.8. 2018	C.8 (C)	11:09:11	11:17:22	491	T1.4	2.42	95.3	+4.8 ±0.9	+1.7 ±0.6
T2.13 (cyan)	23.8. 2018	C.8 (C)	11:39:40	11:46:31	411	T1.4	3.22	75.3	+4.9 ±0.7	+1.0 ±0.4
T2.14 (magenta)	23.8. 2018	C.8 (C)	11:54:35	12:01:45	430	T1.4	2.61	68.6	+5.5 ±0.8	+2.5 ±1.6
T2.15 (yellow)	23.8. 2018	C.9 (C)	13:04:40	13:11:42	423	T1.5	3.03	101.0	+5.6 ±0.8	+3.8 ±0.9

Table S2: UAV2 flight survey details during method testing. The position of the controlled release corresponding to each flight survey is given in brackets after the controlled release number. *P* from a UAV1 flight survey with similar wind conditions is given.

S5 Controlled release details and corresponding UAV aerial flight tracks

CP grade methane (> 99.5% purity; BOC Special Products) was released from either a 10 l or 50 l steel cylinder, filled to approximately 200 bar. A single stage chromium-plated brass regulator with a stainless steel diaphragm (C106X/1B, BOC Special Products) was used to control the line pressure and a mass flow controller (MCR-100SLPM-D, Alicat Scientific, Inc) was used to control the release rate. PFA tubing (0.25" outer diameter), with a length of 50 ft, was used to connect the regulator to the mass flow controller and 100 ft of the same tubing was used to connect the mass flow controller to the release point. The end of this tubing was placed at the bottom of a bucket filled with stones. This ensured that the methane was released at ambient atmospheric temperature.

The date, time and location of each controlled release is given in Table S3, along with F_0. Methane was released on five days; on each day it was released from a fixed position (positions A, B, C, D and E). The position of each release location is given in Figure 1. Each UAV flight track from each controlled release location is given in Figure S10 for UAV1 and Figure S11 for UAV2.

Controlled release	**Date**	**Start time**	**End Time**	**Longitude (° E)**	**Latitude (° N)**	**Position on Figure 1**	F_0/g s^{-1}
C.1	21.8.2018	12:51:00	13:30:00	-2.947005	53.788030	A	0.657
C.2		13:57:00	14:27:00				0.657
C.3		15:26:00	15:57:00				0.657
C.4	22.8.2018	09:57:00	10:25:00	-2.946540	53.787610	B	0.657
C.5		10:30:00	10:40:00				0.657
C.6		11:05:00	11:41:00				0.657
C.7		12:25:00	13:00:00				0.657
C.8	23.8.2018	10:35:00	12:42:00	-2.946855	53.787730	C	1.095
C.9		13:00:00	13:25:00				0.657
C.10	3.9.2018	13:58:00	14:25:00	-2.944920	53.787993	D	0.657
C.11		14:57:00	15:40:00				0.657
C.12		16:03:00	16:34:00				0.657
C.13	4.9.2018	11:44:00	12:13:00	-2.944524	53.788288	E	0.657

Table S3: The duration of controlled methane release from one of five locations, plotted in Figure 1.

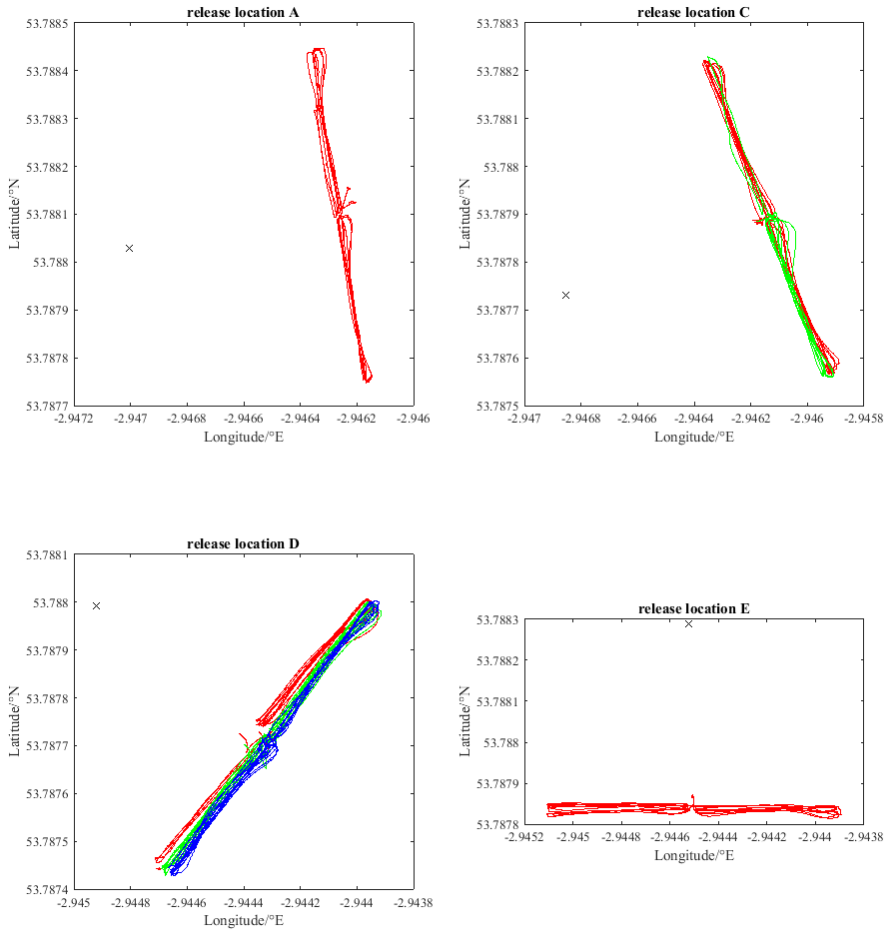

Figure S10. Aerial plots of UAV1 flight tracks (coloured dots), according to each controlled release location (black cross). The colour of each flight track is given in Table S1 and the release location labels are assigned in Table S3.

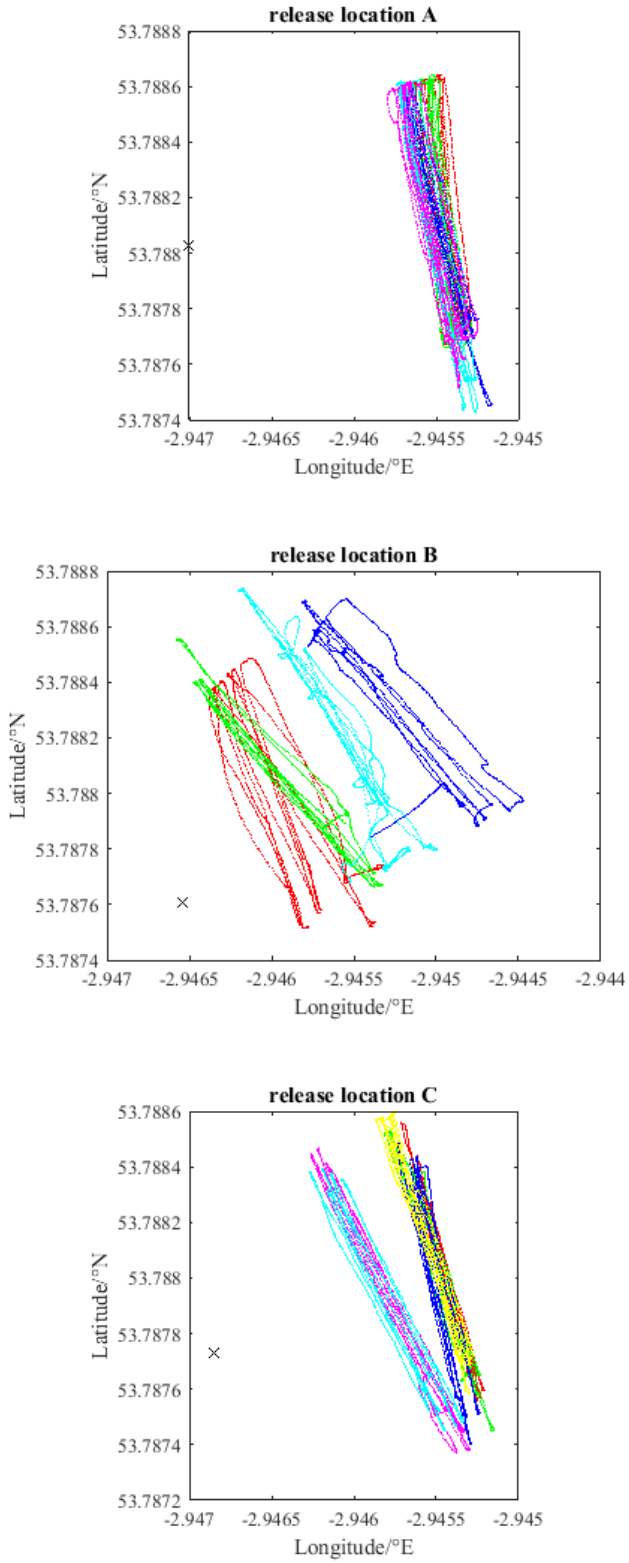

120 **Figure S11. Aerial plots of UAV2 flight tracks (coloured dots), according to each controlled release location (black cross). The colour of each flight track is given in Table S2.**

S6 Wind profiles and uncertainties

Wind speed and direction measurements from wind sensor mounted on UAV1, were used to calculate the wind component, perpendicular to the orientation of the sampling plane, as a function z ($WS^{UAV}(z)$). $WS^{UAV}(z)$ was fitted using Eq. (A) for the full duration of each UAV1 flight survey. $WS^{UAV}(3.3)$ is $WS^{UAV}(z)$ derived at 3.3 m and P is the wind power (see Table S4 for values).

(A) $$WS^{UAV}(z) = WS^{UAV}(3.3) \cdot \left(\frac{z}{3.3}\right)^{P}$$

Each "j" wind residual (WR), between measured $WS^{UAV}(z)$ values and those predicted by Eq. (A), were used to derive the UAV wind uncertainty (ΔWS^{UAV}), using Eq. (B).

(B) $$\Delta WS^{UAV} = \left(\frac{\sum_{j=1}^{N}(WR_j^2)}{NWR}\right)^{\frac{1}{2}}$$

Wind profiles of $WS^{UAV}(z)$ along with ΔWS^{UAV} during method testing are given in Figure S12.

Flight survey	***P***	$\boldsymbol{WS^{UAV}(3.3)/m\ s^{-1}}$
T1.1	0.090	4.5
T1.2	0.127	5.5
T1.3	0.104	7.7
T1.4	0.213	6.2
T1.5	0.190	5.7
T1.6	0.052	6.4
T1.7	0.222	3.0

Table S4: Coefficients used to fit the wind profiles in Figure S12 to Eq. (A) for each UAV1 flight survey during method testing.

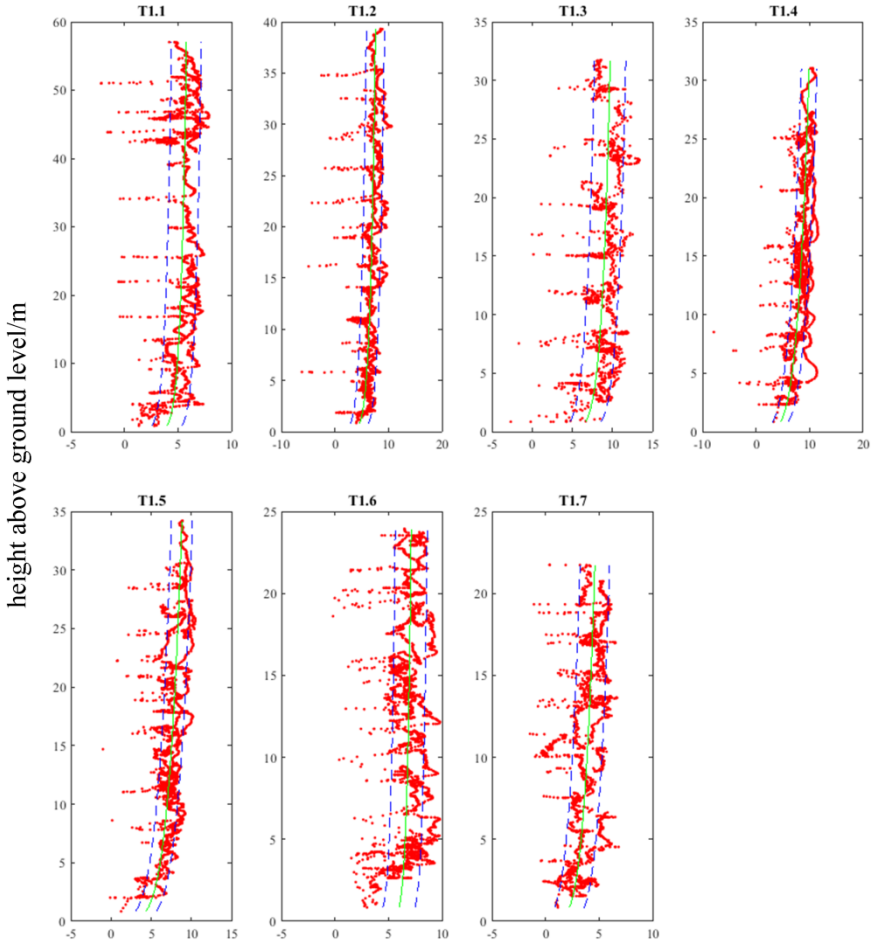

Figure S12. The wind speed component perpendicular to the orientation of the sampling plane, derived from the anemometer mounted on UAV1 (red dots) for each UAV1 method testing flight survey. $WS^{UAV}(z)$ given by Eq. (A) is also plotted (solid green lines), along with corresponding ΔWS^{UAV} bounds from Eq. (B) (dashed blue lines).

The average zonal wind velocity at 3.3 m ($\overline{u(3.3)}$) and the average meridional wind velocity at 3.3 m ($\overline{v(3.3)}$) were derived from measurements made by the stationary anemometer, for the full duration of each flight survey (see Table S1 and Table S2). $\overline{u(3.3)}$ and $\overline{v(3.3)}$ were then used to derive the zonal wind velocity as a function of z ($u(z)$) and meridional wind velocity as a function of z ($v(z)$) using Eq. (C) and Eq. (D), respectively, for the duration of each flight survey.

(C) $$u(z) = \overline{u(3.3)} \cdot \left(\frac{z}{3.3}\right)^{P}$$

(D) $$v(z) = \overline{v(3.3)} \cdot \left(\frac{z}{3.3}\right)^{P}$$

As $WS^{UAV}(z)$ was not measured on UAV2, a wind power was used in Eq. (C) and Eq. (D), corresponding to a flight survey by UAV1 with similar wind conditions, for all UAV2 flight surveys (see Table S2 for choice of P). $u(z)$ and $v(z)$ were combined to derive $WS(z)$ for each flight survey, using Eq. (E).

(E) $$WS(z) = \left(u(z)^2 + v(z)^2\right)^{\frac{1}{2}}$$

NWR is the total number of wind residuals. The uncertainty in $u(z)$ ($\sigma_{u(z)}$) and the uncertainty in $v(z)$ ($\sigma_{v(z)}$) were calculated using Eq. (F) and Eq. (G), respectively.

(F) $$\sigma_{u(z)} = \left(\left(\sigma_{u(3.3)} \cdot \left(\frac{z}{3.3} \right)^{P} \right)^2 + \left(\Delta WS^{\mathrm{UAV}} \right)^2 \right)^{\frac{1}{2}}$$

(G) $$\sigma_{v(z)} = \left(\left(\sigma_{v(3.3)} \cdot \left(\frac{z}{3.3} \right)^{P} \right)^2 + \left(\Delta WS^{\mathrm{UAV}} \right)^2 \right)^{\frac{1}{2}}$$

$\sigma_{u(3.3)}$ is the uncertainty in $\overline{u(3.3)}$ and $\sigma_{v(3.3)}$ is the uncertainty in $\overline{v(3.3)}$, derived from the standard deviation in individual measurements made by the stationary sonic anemometer.

S7 Testing flux results

Flux results and uncertainties for each flight conducted by both UAV1 and UAV2 during the controlled release of methane are given in Table S5.

Flight survey	F_0/g s^{-1}	F_e/g s^{-1}	σ^-/g s^{-1}	σ^+/g s^{-1}	σ_F/g s^{-1}
T2.1	0.657	0.24	0.20	0.27	0.14
T2.2	0.657	0.30	0.27	0.37	0.16
T2.3	0.657	1.44	1.22	1.47	0.80
T2.4	0.657	0.50	0.42	0.52	0.22
T1.1	0.657	0.23	0.21	0.23	0.09
T2.5	0.657	0.89	0.78	0.98	0.42
T2.6	0.657	0.65	0.60	0.84	0.31
T2.7	0.657	0.98	0.78	0.96	0.45
T2.8	0.657	0.57	0.42	0.70	0.22
T2.9	0.657	0.78	0.68	1.07	0.28
T2.10	1.095	0.96	0.77	0.98	0.43
T2.11	1.095	0.95	0.79	1.02	0.46
T2.12	1.095	1.26	1.05	1.29	0.52
T1.2	1.095	1.41	1.23	1.26	0.49
T2.13	1.095	1.49	1.18	1.48	0.75
T2.14	1.095	1.45	1.24	1.61	0.56
T2.15	0.657	0.70	0.61	0.78	0.28
T1.3	0.657	0.22	0.21	0.23	0.07
T1.4	0.657	0.72	0.58	0.63	0.22
T1.5	0.657	1.38	1.17	1.22	0.43
T1.6	0.657	1.00	0.81	0.86	0.39
T1.7	0.657	0.33	0.30	0.31	0.18

Table S5: Known emission fluxes, calculated NGI emission fluxes and flux uncertainty bounds for each UAV flight survey carried out during method testing. The flights are listed in chronologically in order of take-off time.